H-MODE STUDIES IN PDX

By

R.J. Fonck et al.

JULY 1984

PLASMA PHYSICS LABORATORY

PRINCETON UNIVERSITY
PRINCETON, NEW JERSEY

PREPARED FOR THE U.S. DEPARTMENT OF ENERGY,
UNDER CONTRACT DE-AC02-76-CHO-3073

NOTICE

Printed in the United States of America.

Available from:

National Technical Information Service
U. S. Department of Commerce
5285 Port Royal Road
Springfield, Virginia 22151

Price* Printed Copy $ * ; Microfische $3.50

*PAGES	NTIS Selling Price
1-25	$5.00
26-50	$6.50
51-75	$8.00
76-100	$9.50
101-125	$11.00
126-150	$12.50
151-175	$14.00
176-200	$15.50
201-225	$17.00
226-250	$18.50
251-275	$20.00
276-300	$21.50
301-325	$23.00
326-350	$24.50
351-375	$26.00
376-400	$27.50
401-425	$29.00
426-450	$30.50
451-475	$32.00
476-500	$33.50
500-525	$35.00
526-550	$36.50
551-575	$38.00
576-600	$39.50

For documents over 600 pages, add $1.50 for each additional 25 page increment.

PPPL--2110

DE84 015148

H-MODE STUDIES IN PDX[+]

R. J. Fonck, P. Beirsdorfer, M. Bell, K. Bol, D. Boyd,[*] D. Buchenauer,[**] R. Budny, A. Cavallo, P. Couture, T. Crowley, D. Darrow, S. Davis, H. F. Dylla, H. Eubank, R. Goldston, B. Grek, K. Jaehnig, D. Johnson, R. Kaita, S. Kaye, R. Knize, H. Kugel, B. LeBlanc, J. Manickam, D. Manos, D. Mansfield, E. Mazzucato, R. McCann, D. McCune, K. McGuire, D. Mikkelsen, D. Mueller, A. Murdock,[*] M. Okabayashi, K. Okano,[++] D. K. Owens, W. Park, D. Post, M. Redi, M. Reusch, G. Schmidt, S. Sesnic, C. Singer, R. Slusher,[+++] J. Strachan, C. Surko,[+++] H. Takahashi, F. Tenney, H. Towner, M. Ulrickson, and J. Valley,[+++]

Plasma Physics Laboratory, Princeton University, Princeton, NJ 08544 USA

ABSTRACT

A regime of enhanced energy confinement during neutral beam heating has been obtained routinely in the PDX tokamak after modifications to form a closed divertor geometry. Plasma density profiles were broad and the electron temperature at the plasma edge reached values of ~ 400 eV in the H-mode phase of a discharge. A comparison of closed divertor discharges with moderate and intense gas puffing indicates that a requirement for obtaining high confinement times is the localization of the plasma fueling source in the divertor throat region. While high confinement was attained at moderate injected powers ($P_{INJ} \lesssim 3$ MW), confinement was degraded at higher powers due to both increased edge instabilities and, especially, the intense gas puffing needed to prevent disruptions. Initial results with a particle scoop limiter indicate high particle confinement times and energy confinement times approaching those of diverted H-mode plasmas.

[+]Presented at the Fourth International Symposium on Heating in Toroidal Plasmas, Rome, Italy, March 21-1984.

[*]University of Maryland, College Park, MD USA.

[**]IREQ Institut de recherche d'Hydro-Quebec, Canada.

[++]University of Tokyo, Tokyo, Japan.

[+++]Supported by AT&T Bell Laboratories, Murray Hill, NJ USA.

I. INTRODUCTION

During its last seven months of operation from December 1982 to June 1983, the experimental effort on PDX focused on studies of the regime of improved confinement during neutral beam heating in divertor plasmas. This "H-mode" was originally found in diverted ASDEX plasmas /1/. Several modifications to the divertor hardware and the mode of operation of diverted discharges in PDX were made to facilitate routine operation with high confinement plasmas /2/. Earlier experiments on the ASDEX /3/, D-III /4,5/, and PDX /6/ tokamaks and modeling results /7/ suggested that improved power handling could be achieved with a closed divertor configuration in which the only possible path for recombined neutrals in the divertor region to return to the main plasma chamber was through the diverted scrape-off plasma. PDX had typically run in an open divertor configuration, wherein the neutrals could return unimpeded by plasma to the main plasma chamber via open channels near the outer divertor coils. In this open geometry, the neutral gas pressures in the divertor and main plasma chambers were equal, whereas closed divertors, either a mechanical type, such as in ASDEX, or the expanded boundary divertor configuration in D-III, yielded divertor neutral gas pressures of 10-200 times that in the main chamber. Since high confinement was not observed in diverted PDX discharges with neutral injection even though some of the characteristics of the transition to the H-mode were evident, the discovery of the H-mode regime on ASDEX gave additional impetus to modify the PDX divertor hardware in order to close off most of the open conductance paths for neutral gas between the divertor and main plasma chambers. With this and other material and operational changes /2/, diverted plasmas (R_{pl} = 140 cm, a ≈ 40 cm) provided routine access to the ASDEX-like H-mode regime. These closed divertor plasmas had neutral gas compression ratios of 15-30 /8/, and had ~ 3 times less energy deposition on the divertor neutralizer plates than the open divertor cases /9/.

II. CHARACTERISTICS OF THE H-MODE IN PDX DIVERTED DISCHARGES

In general, the transition to the H-mode confinement regime in a diverted plasma is evidenced by a sharp rise in $\bar{n}_e$ despite a constant gas feed rate (t_{trans} = 540 ms in Fig. 1). Prior to this transition, the density is observed to decrease slightly with the onset of NBI, perhaps a reflection of the drop in particle confinement that had been typical of plasma behavior in earlier studies of low-confinement (L-mode) discharges. Concurrent with the rise in $\bar{n}_e$, spontaneous rises in volume average toroidal beta $\langle\beta_T\rangle$ and the total energy confinement time τ_E are observed. The time at which the transition occurs is dependent on the total absorbed power (and indirectly $\bar{n}_e$), with typical threshold values ranging from 1-2 MW. The transition occurs at lower P_{abs} when either I_p or B_T is lowered.

A feature that signals the onset of the H-mode confinement phase of the discharge is a sharp drop of the line-averaged density and the working gas emissions (H_α or D_α) in the divertor region /2,10/, as shown in Fig. 1. This drop in H_α/D_α emission, coupled with the lack of any rise in H_α/D_α emission in the plasma main chamber, a drop in the fast neutral efflux from the plasma core, and constant or reduced impurity content and radiated power at the transition time, indicates a rise in the particle confinement time, τ_p, by a factor of ~ 2. The sharp spikes evident in the H_α/D_α emission after the H-mode transitions are indicative of edge relaxation phenomena (ERP), which are discussed in a later section of this paper. The drop in H_α/D_α emission in the divertor region was taken to be the operational definition of an H-mode discharge in PDX. However, it is only a necessary but not sufficient condition for the achievement of high confinement in a given discharge, and under our definition, H-mode plasmas can be obtained without exhibiting improved confinement.

In the divertor region, several changes in the plasma, in addition to the H_α/D_α drop, occur at the transition to the H-mode. Probe measurements in the divertor plasma show that a drop in T_e and a rise in n_e at the separatrix, along with a drop in the total power flux to the neutralizer plates, all occur at the time of the transition /11/. Both electron and power density profiles in the divertor region become more peaked than in the L-mode phase of the discharge. While the total power flux to the neutralizer plate during the quiescent H-mode phase is less than that observed for the L-mode phase of the discharge by 30% or more, it does not drop to zero, indicating that total plugging of energy flow into the divertor region is not necessary for high confinement.

In addition to the drop in fast neutral efflux mentioned earlier, the power flow along the field lines several centimeters outside the separatrix in the main plasma chamber decreases at the onset of the high confinement phase, reflecting increased gradients at the plasma edge. Most striking, perhaps, is the rapid rise in electron temperature at a location of a few centimeters inside the separatrix (R_{sep} = 180 cm) in the main plasma (Fig. 1b). This rise in T_e and the H_α/D_α drop in the divertor often follow a sawtooth oscillation of the main plasma, suggesting that the heat pulse propagating out of the plasma center to the edge aids in triggering the H-mode onset. Transitions of the H-mode are also observed in the absence of sawtooth activity, but under these circumstances, the rise in $T_e(R = 176)$ is slower ($\tau_{Rise} \sim 3$ ms) than in the case with sawteeth ($\tau_{Rise} \sim 0.3$ ms). A study of ~ 25 discharges in PDX without sawteeth indicates that there is no simple threshold in edge T_e for transition to the H-mode, and values of $T_e(R = 176)$ from 200 to 550 eV are observed prior to the transition.

Transitions to the H-mode phase, coupled with improvement in overall confinement of the discharge, were observed over a wide range of operating

parameters in PDX. For example, plasmas with I_p = 200-490 kA, B_T = 0.9-2.1 T, β_p = 0.4-1.4, $\langle\beta_T\rangle$ = 0.9-2.4%, P_{INJ} = 1-5 MW, and Z_{eff} = 2-4 all displayed H-mode characteristics. Also, values of q(a) = 2-7 were achieved in H-mode plasmas with no observed trouble passing through the q = 3 barrier. H-mode plasmas were obtained with a variety of beam and plasma species (i.e., $D^\circ \rightarrow D^+$, $H^\circ \rightarrow D^+$, $D^\circ \rightarrow He^{++}$), but the most favorable results were obtained with $D^\circ \rightarrow D^+$, and most of the experiments reported here concentrated on this case.

Electron density and temperature profiles, obtained with a 56-channel Thomson scattering system, are shown in Fig. 2 for times prior to the H-mode and well after the H-mode transition, near the peak of the density rise. Density profiles typically broaden just after the transition, and while the electron temperature profiles sometimes broaden they always develop high edge temperatures (~ 400 eV) for good H-mode discharges. Often, as in Fig. 2, the T_e profile appears to gain a "pedestal," or constant addition, of 200-300 eV at all radii. Likewise, observations on $H^\circ \rightarrow D^+$ discharges have shown that both the ion temperature and toroidal rotation velocity profiles broaden considerably after transition into the H-phase of the discharge, indicating an improvement in toroidal momentum confinement in addition to increases in particle and energy confinement.

The edge of the plasma was studied in more detail with a single point Thomson scattering system designed for low T_e measurements. Profiles of n_e and T_e at the plasma edge, as seen in Fig. 3, show very sharp gradients (~ 200-300 eV/cm and ~ 3 x 10^{13} cm^{-3}/cm) near the separatrix in a well-developed H-mode discharge. The shaded regions in Fig. 3 indicate our best estimates to date of the position of the separatrix for these discharges. The position was determined by MHD equilibrium calculations that use the externally applied fields, I_p, flux measurements, eddy current corrections, peak plasma pressure, and estimates of ℓ_i and β_p to model the measured plasma pressure and current

density (assuming $j_\phi \propto T_e^{3/2}$). A modified Grad-Shafranov equation which includes the centrifugal effects of toroidal rotation was used to obtain a reasonable match to the outward asymmetry of the pressure profile (c.f. Fig. 2,. However, the required rotation velocity was up to 3 times greater than the value measured. An exhaustive survey of such calculations of model functions to test the sensitivity of the separatrix location to uncertainties in the input parameters is still in progress. However, it appears that the sharp gradients in the plasma profiles occur inside the separatrix. This being the case, the measurements of the electron density and temperature outside the separatrix in the plasma midplane, combined with probe measurements of the same quantitites in the divertor chamber, show that the parallel gradient in T_e from the main chamber midplane to the divertor region can be supported by classical flux-limited thermal conduction along the field lines.

III. ENERGY CONFINEMENT SCALING AND TRANSPORT

Studies of the dependence of total energy confinement times on various discharge parameters show that τ_E^{eq}, the magnetics equilibrium value of the total energy confinement time, depends principally on the total plasma current in H-mode discharges, just as it does for L-mode plasmas /12,13/. Typically, $\tau_E \sim I_p/8\text{-}11$ for high confinement H-mode (diverted) cases and $\tau_E \sim I_p/15\text{-}30$ for L-mode (limiter) cases. The difference between the diverted and limiter plasmas may be partially due to the target plasma in the circular case being hydrogen instead of deuterium. Depending on the actual isotope mix in the plasma during NBI, this isotope difference could account for perhaps a factor of 1.4 increase in τ_E^{eq} for the diverted case /14/.

In general, we use a discharge confinement quality factor, defined as τ_E/I_p (τ_E in msec, I_p in kA), to remove the I_p dependence of τ_E in order to study the dependence of τ_E on other parameters. It was found that τ_E/I_p did

not depend on the toroidal field strength and displayed no explicit dependence on $\bar{n}_e$, although the actual density range studied was relatively narrow (3-6 x $10^{13}cm^{-3}$). At best, values of τ_E^{eq}/I_p up to 0.14 msec/kA were observed in PDX. The behavior of τ_E/I_p as a function of total input power, (P_{OH} + P_{ABS}), Fig. 4, shows that significantly enhanced H-mode confinement is achieved only at modest values of P_{Total}. The variability in the H-mode data at $P_{Total} \sim 2$ MW arises from variations in the operating conditions (e.g., amount of gas puffing used, vertical plasma position, etc.) and in the occurrence of the edge relaxation phenomena mentioned earlier. The shaded area in Fig. 4 shows the range of τ_E/I_p achieved for $D^o \rightarrow H^+$ discharges formed on a carbon rail limiter.

It is especially interesting to note that no reasonably high confinement discharges were obtained for $P_{Total} \gtrsim 3$ MW. The residual improvement above the limiter discharges for high P_{Total} may be due to the isotope effect. The cause of the degradation in confinement at high input powers is not completely understood, but at least two effects may contribute. First, the edge relaxation phenomena (ERP) characterized by sharp spikes in the edge H_α/D_α emission are known to cause rapid decreases in the energy stored in the outer half of the plasma /2,10/ and these ERP's appear to become more intense and frequent as the input power increases. Indeed, the best confinement was often achieved in a narrow range of P_{INJ} where enough power was available to induce the transition to the H-mode but not enough to cause serious ERP's. However, it is difficult to evaluate quantitatively the effects of the ERP's on the total confinement due to the sensitivity of the H_α/D_α excitation to varying edge conditions. Second, and probably more important, it was necessary to increase the gas feed rate in the divertor dome by at least a factor of 3 in order to avoid disruptions when the injected power was above ~ 3 MW. It will be shown in a later section of this paper

that increased gas puffing results in a loss of H-mode confinement even at low P_{INJ}. For some of the high P_{Total} data, the increased gas feed was required to reduce the metallic impurity influx, principally iron, which otherwise would lead to hollow temperature profiles and disruptions. The source of the iron contamination was not positively identified, but most likely was the stainless steel liners surrounding the divertor throat. Whether this impurity contamination problem was present for all the shots with high P_{Total} is still under evaluation. The few shots at $P_{INJ} > 3$ MW which went through with no disruption and no increased gas puffing also did not show high confinement, but our results do not definitely rule out the possibility of higher τ_E/I_p at high P_{INJ}.

The energy transport of H-mode discharges was analyzed with the time-dependent transport analysis code TRANSP /15/. Thomson scattering profiles of the plasma T_e and n_e were taken at several times throughout the discharge to produce a temporal evolution of the plasma profiles. Analyses of several cases indicate that the dominant plasma energy loss is through the electron channel, just as it is for L-mode discharges, and this loss is attributed to anomalous electron thermal conduction. The dominant energy loss for ions is through coupling to the electrons, and the ion thermal conductivity is typically 1 to 3 times the Chang-Hinton neoclassical value in order to match the measured central ion temperature. Sample results from the transport analysis are shown in Fig. 5, which show the total thermal energy confinement time as a function of time in the discharge and the electron thermal diffusivity as a function of radius for the L- and H-mode phases of the discharge. The drop in the thermal confinement time at the onset of neutral injection is typical of the transition from ohmic to neutral beam heating in L-mode discharges. The sharp increase in τ_E at the H-mode transition is

similar to that seen in the τ_E^{eq} values. This rise is much faster than the increase in $\bar{n}_e$ and it arises primarily from the increase in the total stored energy, as evidenced by development of the "pedestal" in the T_e profile, and from a decrease in the electron thermal diffusivity, χ_e, over a large part of the plasma, as indicated in Fig. 5. The reduction in χ_e results mostly from the rise in n_e since the gradients in T_e change little in the L- to H-mode transition. However, it should be noted again that there is no explicit dependence of τ_E on $\bar{n}_e$ during the equilibrium phase of the discharge. Finally, the transport analysis indicates that there is a drastic reduction in the particle outflow at the edge ($r/a = 3/4$) near the time of the transition, resulting in an increase in n_e there that is comparable to the ionization source rate of thermal neutrals in that outer region.

IV. MHD ACTIVITY AND FLUCTUATIONS IN H-MODE PLASMAS

Two types of MHD and fluctuation activity were uniquely associated with the H-mode phase of a discharge. The first was a quasicoherent density oscillation which was observed by CO_2 laser scattering and microwave scattering experiments in the 50-100 kHz range having zero amplitude outside the separatrix but rising sharply inside the separatrix /16,17/. This localized mode at the plasma edge occurred in bursts of ~ 300 μs and it persisted throughout the H-mode phase of the discharge.

The second instability associated with H-mode plasmas is the previously mentioned edge relaxation phenomena (ERP), which was characterized by a sharp spike in the edge H_α/D_α signal. Seen on all edge signals, such as H_α/D_α emissions, soft X-ray emissions at large radii, and divertor density measurements, these oscillations are sawtooth-like relaxation modes on the outer half of the plasma with an inversion radius at the plasma edge , as seen in Fig. 6. The presence of these bursts are correlated with decreases in $\bar{n}_e$,

τ_p, τ_E, and $\langle\beta\rangle$, along with an increase in the parallel power flow outside the separatrix. During an ERP, the H_α/D_α emission increased around the entire plasma in the main chamber, and the angular distribution of the fast neutral flux from the plasma was consistent with an increase in the background neutral density in the main plasma. The ERP's appear to affect the thermal plasma rather than the slowing-down fast ions. The presence of this mode results in an abrupt loss of stored energy from the plasma, and, as mentioned earlier, this instability clamps the rise in average τ_E achievable in H-mode discharges. When these bursts disappeared in the course of an H-mode discharge, the $\langle\beta_T\rangle$, $\tilde{n}_e$, and τ_E were subsequently observed to rise. The best confinement times are invariably observed in discharges that did not have this instability present.

The relative amplitude of the D_α bursts (i.e., $\delta D_\alpha(\text{rms})/D_\alpha$) increase with increasing I_p and $\dot{I}_p$, and it is noted that H-mode plasma profiles, with their relatively broad T_e and current density profiles, are calculated to be more unstable to surface kink modes than L-mode plasmas. Indeed, a poloidal array of Mirnov coils often shows a possible surface kink precursor oscillation with (m, n) = (3,0) or (3,1), which appears strongest at the X-point region near the divertor throat. Simultaneous observation at different toroidal locations show the ERP's to have a helical nature, propagating toroidally in the ion diamagnetic direction.

In general, the level of broadband turbulence produced by electron density fluctuations in the range of 50-500 kHz was lower for H-mode plasmas than that observed previously in limiter plasmas with neutral beam heating. However, this observed reduction in $\tilde{n}/\bar{n}$ is caused primarily by an increase in $\bar{n}_e$ after the H-mode transition rather than by a decrease in the density fluctuation level $\tilde{n}$. Discrete MHD activity such as sawteeth and "fishbone"

oscillations /18/, which had previously been observed routinely in PDX, was often present in H-mode discharges also. Interestingly, ERP's decrease the amplitude of the fishbone oscillations as observed with magnetic loops at the plasma edge.

V. ROLE OF THE DIVERTOR IN H-MODE CONFINEMENT

In an effort to understand the improvement in confinement achieved by closing the divertor region and the degradation in confinement with intense gas puffing (as was needed for high P_{INJ}), a series of measurements was made varying both the plasma vertical position and the gas puffing geometry (i.e., midplane or upper divertor gas puffing) and intensity. A clear positive dependence of τ_E^{eq} on the neutral gas compression ratio, P_{DIV}/P_{MAIN}, was discovered, and was due primarily to variations in P_{MAIN}, as shown in Fig. 7. With increasing P_{MAIN}, τ_E^{eq} degrades from $\sim I_p/10$ to $I_p/20$. Nevertheless, all these discharges exhibit the distinctive drop in D_α in the divertor region. Those with low τ_E^{eq} show a rapid recovery of the D_α level or even an increase above the pretransition level. The importance of reducing neutral gas recycling in the main plasma chamber, reflected by the behavior of the neutral pressure or D_α emission, was subsequently confirmed in comparisons of limiter and divertor discharges on the D-III tokamak /19/.

A similar dependence of τ_E on P_{MAIN} also holds for discharges with a single null and divertor dome gas puffing (i.e., standard H-mode conditions), but with intense gas puffing (e.g., 150 Torr - ℓ/sec versus ~ 20 Torr - ℓ/sec for a good H-mode). With such intense gas puffing, the plasma density is sometimes forced to rise up to or above a level to which it would naturally evolve in the course of a good confinement H-mode discharge. In this forced density rise case, however, both the divertor and midplane D_α signals rise rapidly during NBI, indicating that the plasma recycling and refueling source

has moved into the main chamber. This is seen dramatically in D_α emission contours measured with the large aperture Thomson scattering optics, as shown in Fig. 8. The high confinement H-mode discharge, with a constant gas feed, exhibits good particle and energy confinement while the D_α emission and hence the plasma particle source is quite localized near the divertor throat. The particle source is significantly delocalized for the large gas puff case with low confinement. At the same time, the plasma density and temperature gradients at the plasma edge drop from values similar to those in Fig. 3 to ~ 8.5×10^{12} cm^{-3}/cm and 90 eV/cm, respectively. The value of T_e at a position of ~ 4 cm inside the separatrix drops from ~ 500 eV in the good confinement H-mode plasma to ~ 350 eV in the forced density rise case /2/. This value is still considerably higher than that seen in the L-mode plasmas, suggesting that high edge T_e alone does not assure good confinement.

A reexamination of earlier open divertor experiments with neutral beam heating has shown that the characteristic sharp drop in H_α/D_α emission from the divertor region did indeed occur in the open divertor cases with sufficient absorbed beam power. In most cases, however, no improvement in particle confinement occurred and the plasma density could be sustained only by increased gas puffing. Hence, the H_α/D_α emissions were often similar to the forced density rise case in the closed divertor, and no improvement in the energy confinement was evident. The transitions to the H-mode in the open divertor configuration were most pronounced during a short run with $D^o + D^+$ plasmas and with no gettering in the upper divertor region. In this case, the drop in D_α in the divertor region was noticeable and the discharge subsequently developed the edge relaxation instabilities which are characteristic of H-mode plasmas. In a few cases, a rise in $\bar{n}_e$ and τ_E is evident at the time of the L- to H-transition, but the ultimate confinement

quality was still only ~ $I_p/20$. Thus, while the divertor plasma always shows the characteristic transition above some threshold input power whether the divertor is open or closed, improved confinement appears to depend upon the control and localization of the neutral particles and plasma fueling source.

VI. CONFINEMENT WITH A PARTICLE SCOOP LIMITER

The H-mode results in diverted plasmas emphasize the importance of controlling the fueling and neutral particles in the discharge. If this is the salient feature for attaining improved confinement with auxiliary heating, there is a possibility that high confinement may be achieved without a divertor. To explore this possibility, a series of discharges was formed using a particle scoop limiter as the primary limiter. A detailed description of this limiter and some of its performance characteristics have been given elsewhere /20/, and we summarize here only the relevant confinement results.

During NBI, the plasma density rose continuously while the D_α emission on the plasma midplane toroidally separated by 120° from the scoop did not rise, indicating a very localized fueling source and/or improved particle confinement times compared to earlier rail limited discharges. Neutral gas pressures in the scoop plenum were ~ 10^{-2} Torr while the pressure immediately outside the scoop region was ~ 10^{-5} Torr. Plasma TV observations of the scoop showed low levels of visible light localized near the scoop blades. In addition, the fast neutral charge-exchange flux from the plasma near the limiter, as measured with a horizontally scanning charge-exchange analyzer, was at most ~ 1/3 of the level observed in H-mode plasmas and even lower still than that observed with a conventional rail limiter plasma. Comparisons between the measured flux spectra with that calculated by TRANSP imply particle confinement times of > 100 ms. It is clear that the scoop limiter had a significant effect on the particle confinement and fueling properties of

these discharges.

Plasma electron temperature and density profiles for a typical scoop limiter discharge with neutral beam injection are shown in Fig. 9 for P_{INJ} = 2.3 MW, $D^0 \rightarrow D^+$. Large radial gradients in n_e and T_e exist just outside the field of view of the Thomson scattering system (note that R_{Lim} = 193 cm). Extrapolations of the radial profile of parallel power flow at the plasma edge, as measured with a calorimeter probe in the limiter shadow and infrared TV observation of the pump limiter surface, are consistent with the values inferred from the profiles in Fig. 9.

While no transition to a higher confinement regime was obvious for these discharges, the discharge confinement quality factor τ_E^{eq}/I_p was intriguingly similar to that observed for the diverted H-mode plasmas, as shown in Fig. 10. Although the data set is relatively sparse, there does appear to be a regime, at least at $P_{TOTAL} \lesssim 3$ MW, wherein the confinement quality is enhanced above those obtained with a rail limiter. The values of τ_E^{eq} derived from the magnetics analysis were confirmed by evaluation of the thermal τ_E using TRANSP. The confinement quality showed no obvious dependence on Z_{eff} or $\bar{n}_e$. No reason for the drop in τ_E/I_p at high P_{Total} has been found, and further investigation is needed.

VII. SUMMARY

The regime of high confinement during neutral beam injection into divertor discharges, which was originally observed on ASDEX, has been attained routinely on PDX after the divertor geometry was modified to inhibit the backflow of neutral hydrogen from the divertor chamber to the main plasma chamber. The quality of the confinement in a given H-mode discharge is related to the edge plasma properties and apparently depends on the ability to control neutrals and the location of the plasma fueling source. Intense gas

FIGURE CAPTIONS

Fig. 1. Variations in edge plasma parameters during an H-mode discharge. (a) Line-averaged density in plasma midplane. (b) $T_e(t)$ at a position of ~ 4 cm inside the separatrix in the plasma midplane, as measured via second harmonic electron cyclotron emission. (c) D_α emission in plasma midplane. (d) D_α emission from divertor region. The H-mode transition is at t = 530 msec.

Fig. 2. Electron temperature and density profiles from Thomson scattering for the L- and H-mode phases of a high confinement discharge.

Fig. 3. Electron temperature and density profiles at the outer edge of the plasma for a high confinement discharge. The shaded regions indicate the estimated location of the separatrix as determined from an MHD equilibrium code.

Fig. 4. Normalized total energy confinement time as a function of total input power $(P_{INJ} + P_{OH})$ for H-mode discharges. The shaded region denotes the range of τ_E^{eq}/I_p obtained for L-mode discharges obtained with a graphite limiter.

Fig. 5. Kinetic transport analysis results for an H-mode discharge. (a) Total thermal confinement time as a function of time; (b) comparison of the electron thermal diffusivity for the pretransition (L-mode) and H-mode phases of the discharge.

Fig. 6. (a) Soft X-ray emissions as a function of chordal height in the plasma during the H-mode phase of the discharge. (b) Divertor H_α/D_α signal for the case shown in (a).

Fig. 7. Dependence of total energy confinement time on midplane neutral gas pressure for H-mode plasmas.

Fig. 8. H_α/D_α emission contours (in relative units) in a poloidal cross section for: (a) a standard high confinement H-mode plasma, and (b) an H-mode plasma with a forced density rise induced by intense gas puffing in the divertor region. The plasma separatrix is noted by the dashed line.

Fig. 9. Thomson scattering profiles of scoop limiter plasmas. $R_{p\ell}$ = 155 cm and R_{Lim} = 193 cm. The Thomson scattering system is located ~ 140° toroidally away from the limiter.

Fig. 10. Confinement quality factor as a function of total input power for D° + D^+ scoop limiter plasmas.

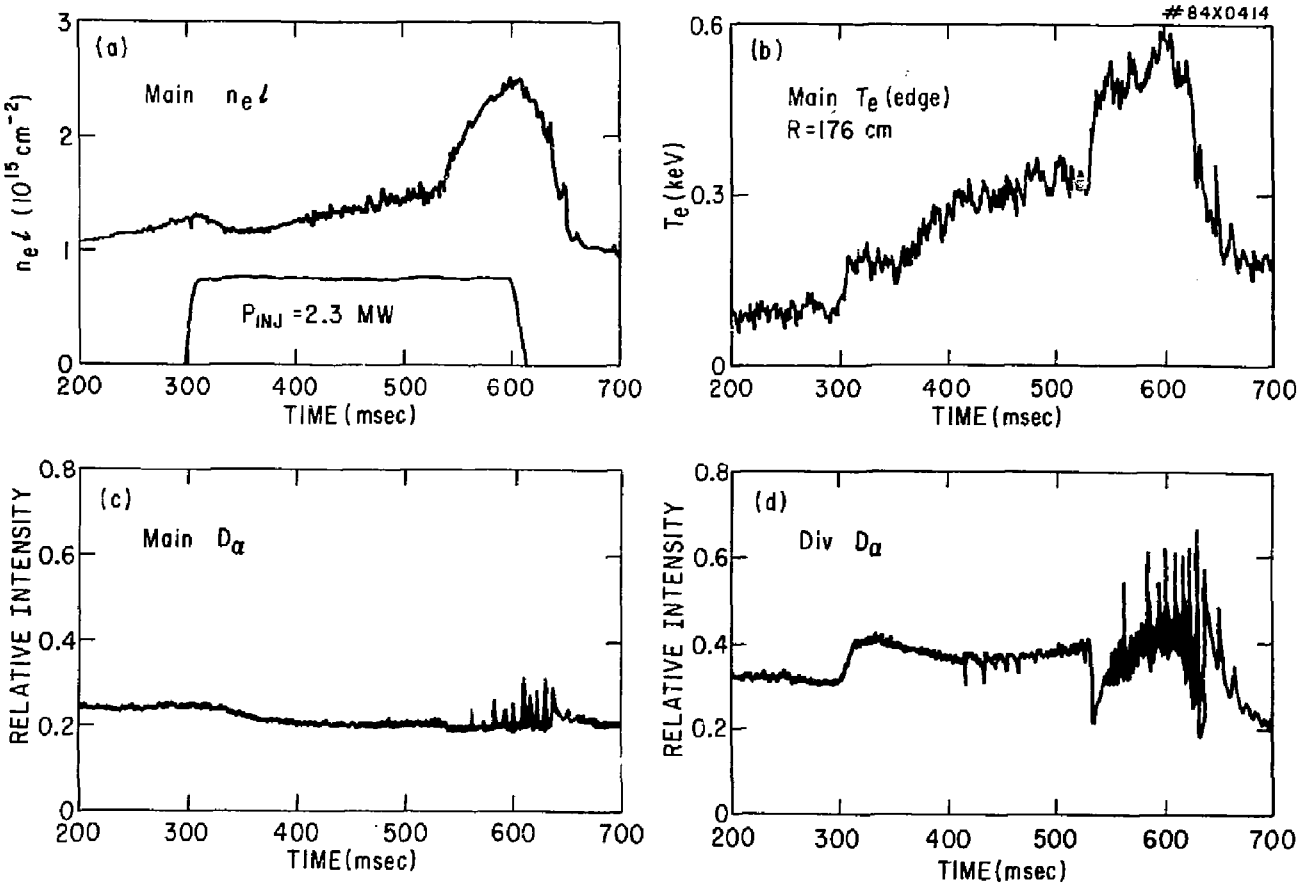
#84X0414
(a)
Main $n_e \ell$
P_{INJ} =2.3 MW
$n_e \ell$ (10^{15} cm^{-2})
TIME (msec)
(b)
Main T_e (edge)
R=176 cm
T_e (keV)
TIME (msec)
(c)
Main D_α
RELATIVE INTENSITY
TIME (msec)
(d)
Div D_α
RELATIVE INTENSITY
TIME (msec)

Fig. 1

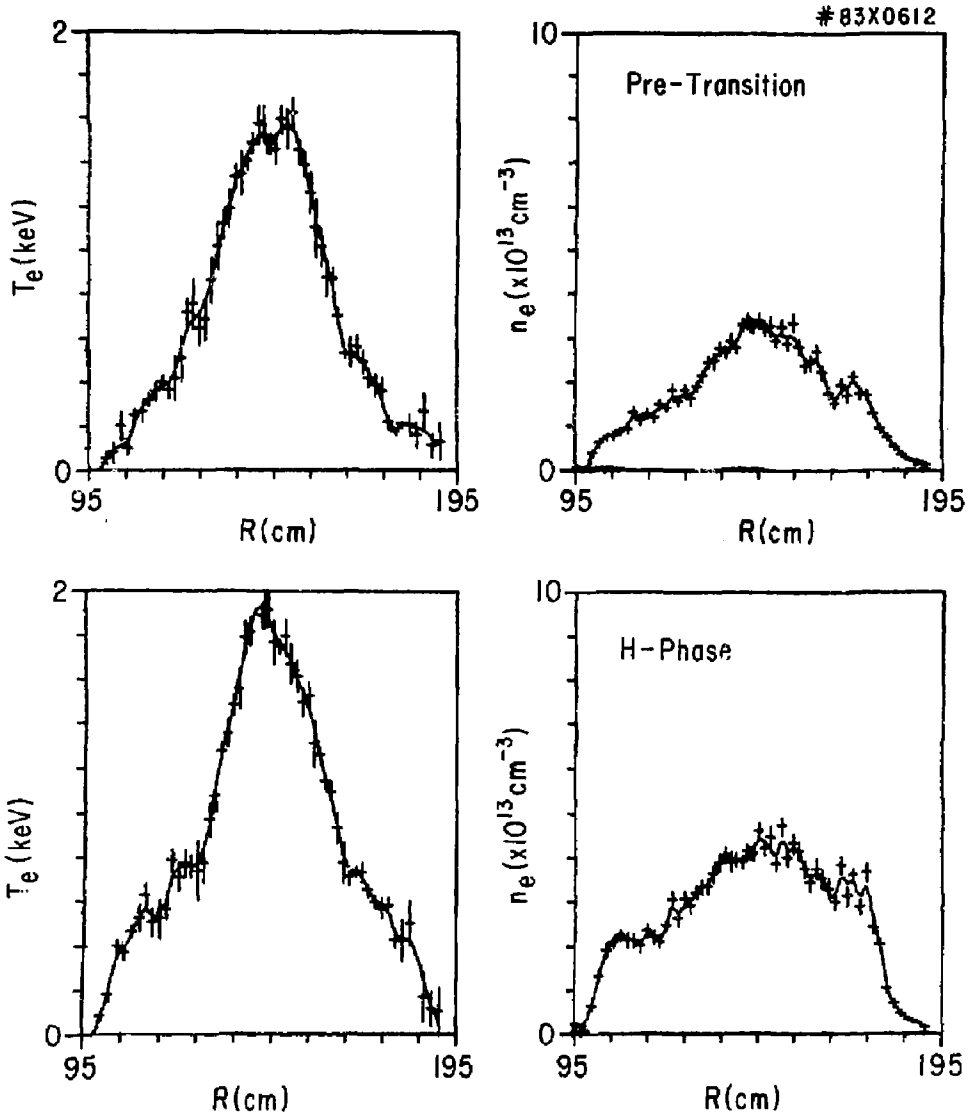
#83X0612
Pre-Transition
H-Phase
T_e(keV)
n_e(x10^{13}cm^{-3})
R(cm)
2
0
10
95
195

Fig. 2

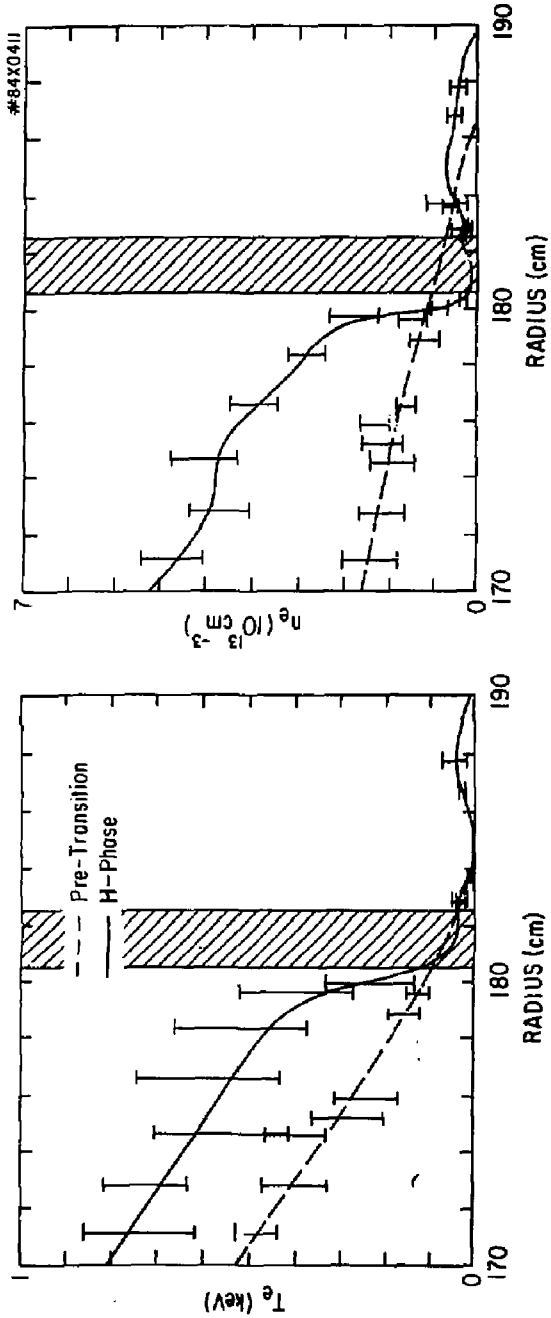
#84X0411
n_e (10^{13} cm^{-3})
7
0
170
180
190
RADIUS (cm)
T_e (keV)
1
0
Pre-Transition
H-Phase

Fig. 3

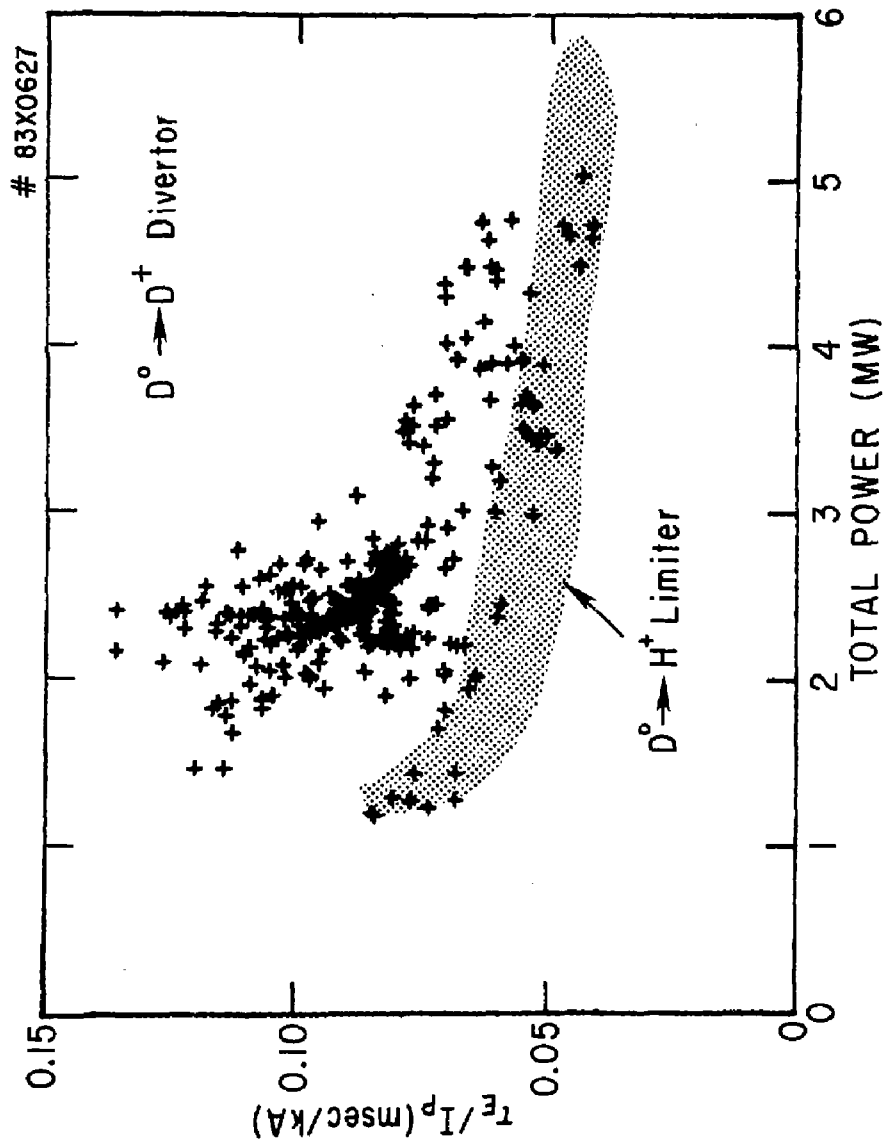
83X0627
D°→D⁺ Divertor
D°→H⁺ Limiter
τ_E/I_p (msec/kA)
0.15
0.10
0.05
0
0
1
2
3
4
5
6
TOTAL POWER (MW)

Fig. 4

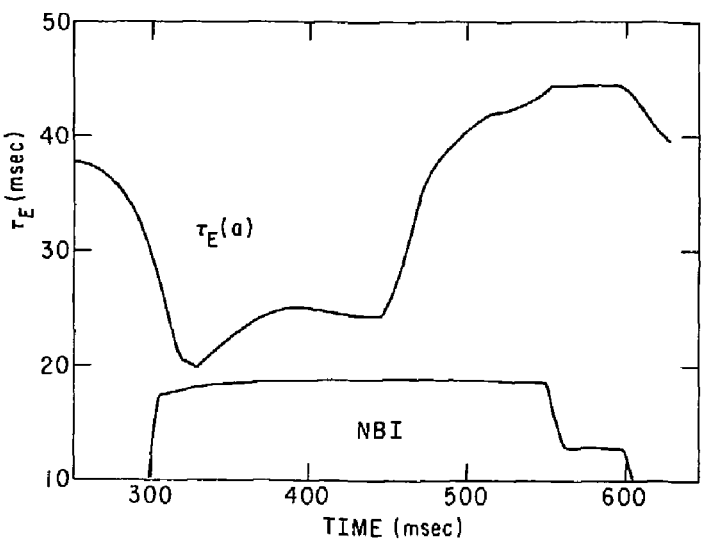
50
40
30
20
10
τ_E (msec)
$\tau_E(a)$
NBI
300
400
500
600
TIME (msec)

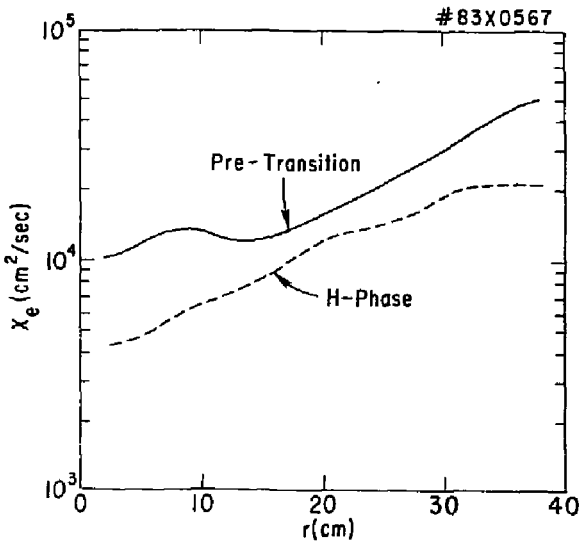
#83X0567
10^5
10^4
10^3
χ_e (cm^2/sec)
Pre-Transition
H-Phase
0
10
20
30
40
r(cm)

Fig. 5

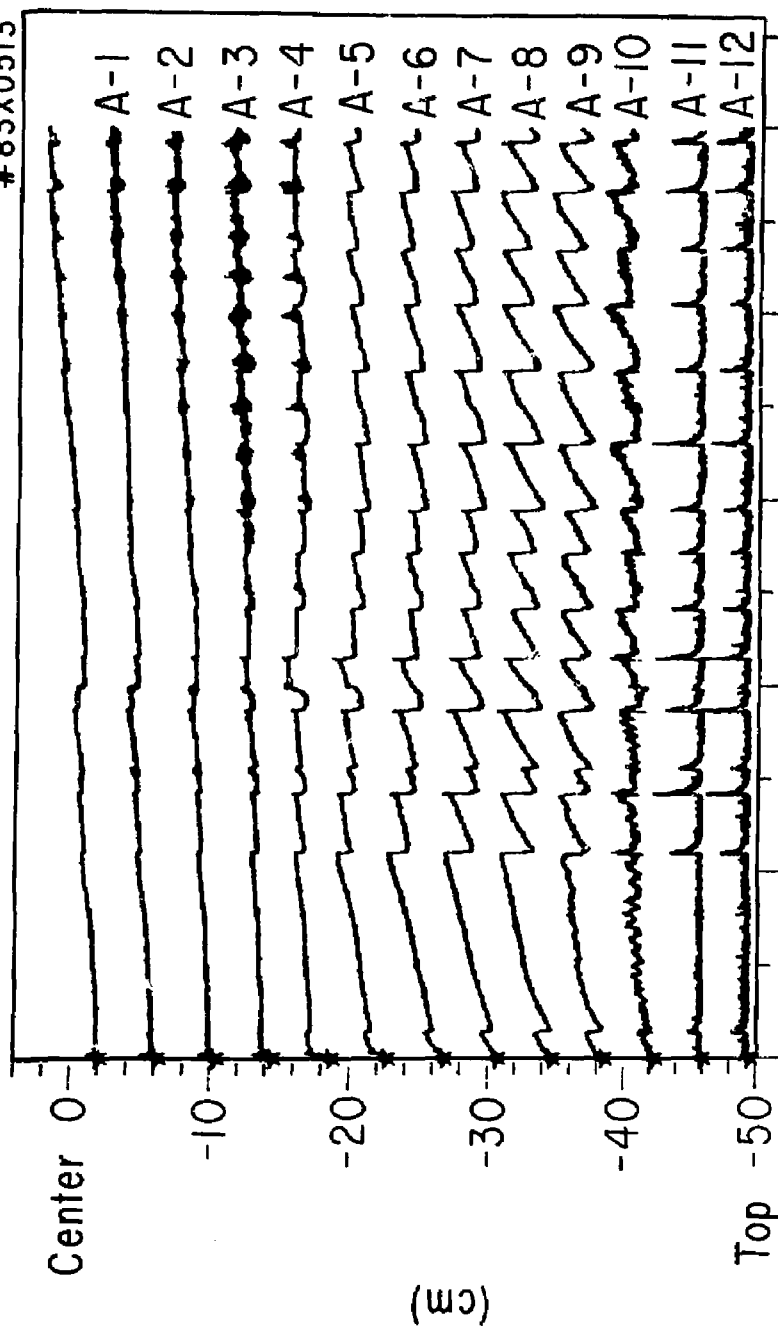
#83X0513
A-1
A-2
A-3
A-4
A-5
A-6
A-7
A-8
A-9
A-10
A-11
A-12
Center 0
-10
-20
-30
-40
Top -50
(cm)
460
480
500
520
540
560
TIME (msec)

Fig. 6(a)

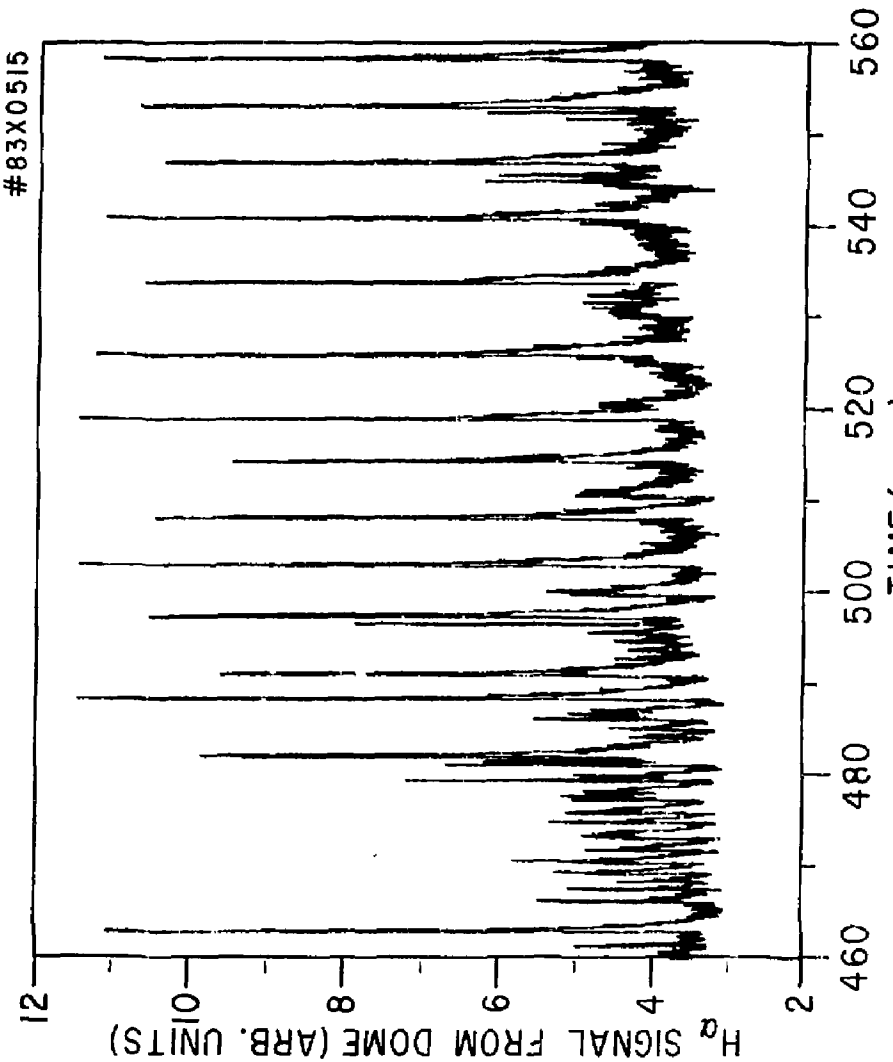
#83X0515
H_α SIGNAL FROM DOME (ARB. UNITS)
12
10
8
6
4
2
460
480
500
520
540
560
TIME (msec)

Fig. 6(b)

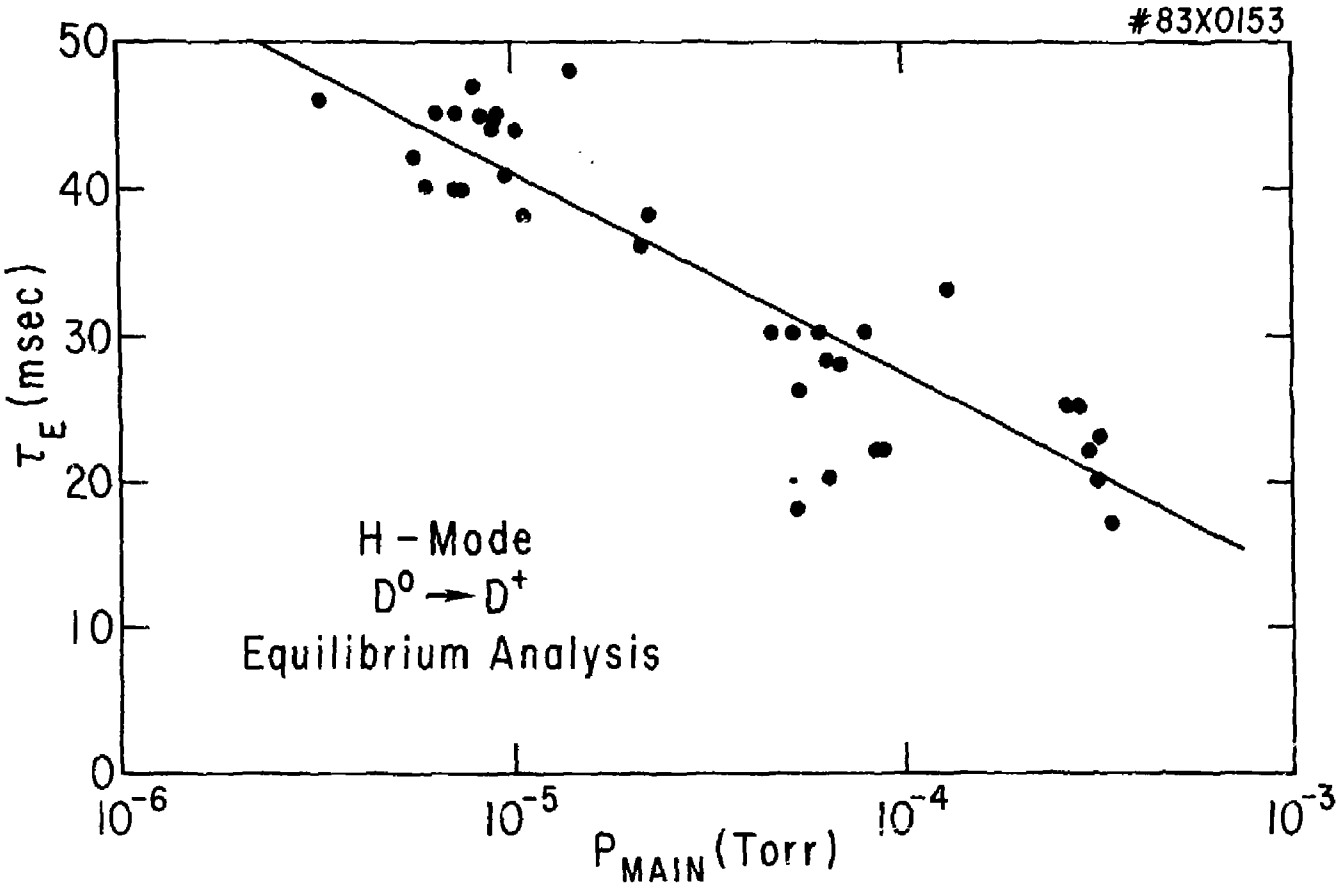
#83X0153
50
40
30
20
10
0
τ_E (msec)
H - Mode
$D^0 \rightarrow D^+$
Equilibrium Analysis
10^{-6}
10^{-5}
10^{-4}
10^{-3}
P_{MAIN} (Torr)

Fig. 7

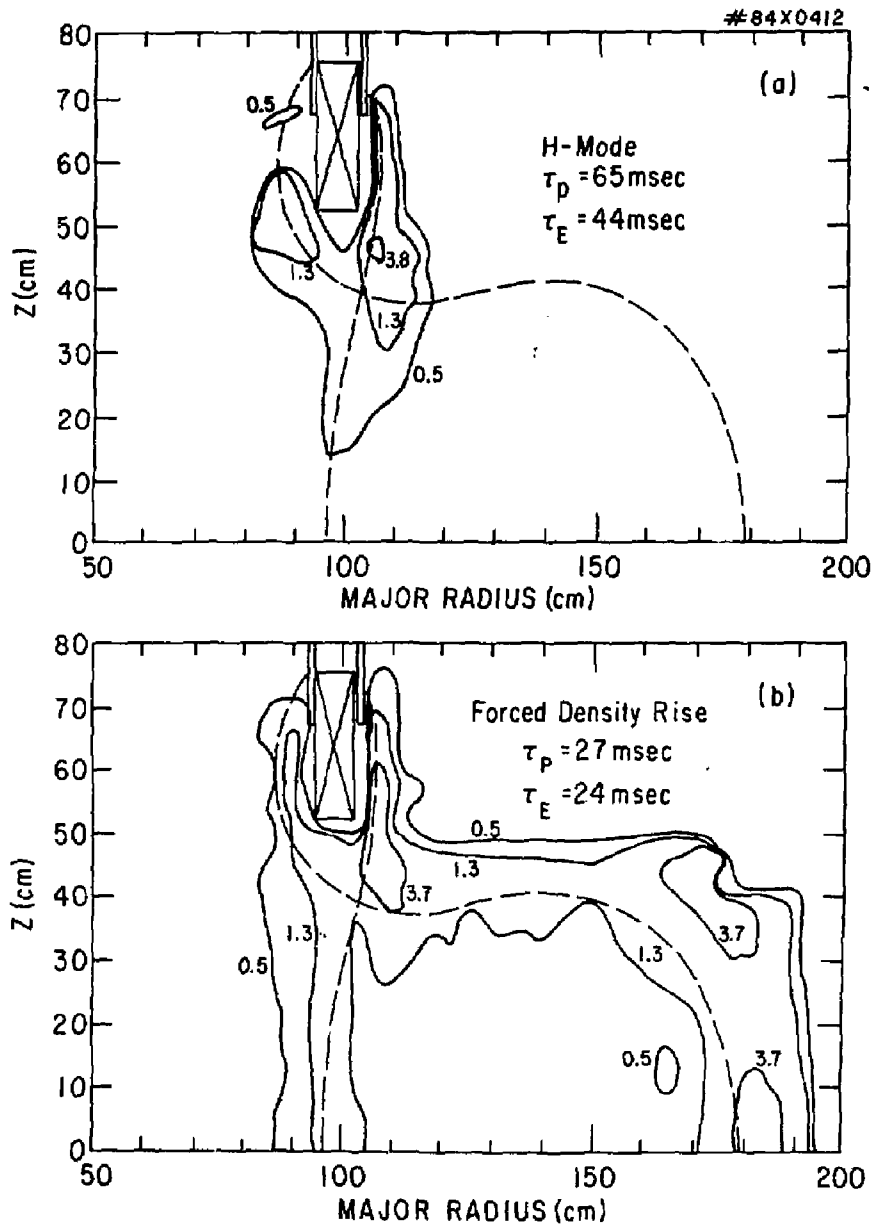
#84X0412
(a)
H-Mode
τ_p =65msec
τ_E =44msec
0.5
1.3
3.8
1.3
0.5
Z(cm)
MAJOR RADIUS (cm)
(b)
Forced Density Rise
τ_P =27msec
τ_E =24msec
0.5
1.3
3.7
1.3
0.5
3.7
1.3
0.5
3.7
Z (cm)
MAJOR RADIUS (cm)

Fig. 8

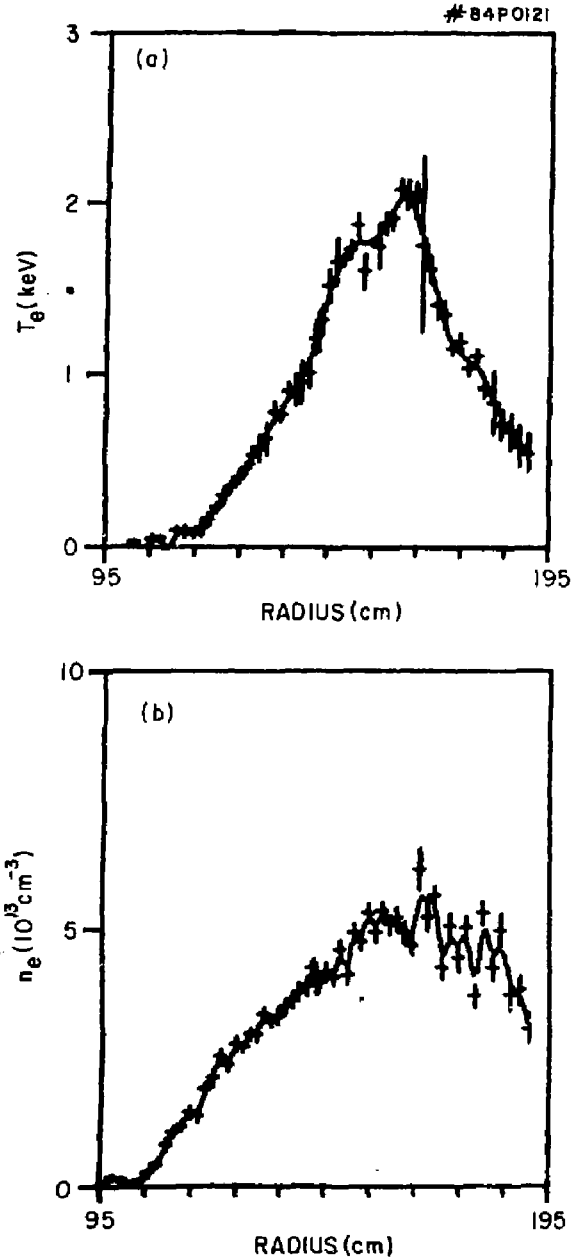
#84P0121
(a)
3
2
1
0
T_e(keV)
95
195
RADIUS(cm)
(b)
10
5
0
$n_e(10^{13}cm^{-3})$
95
195
RADIUS(cm)

Fig. 9

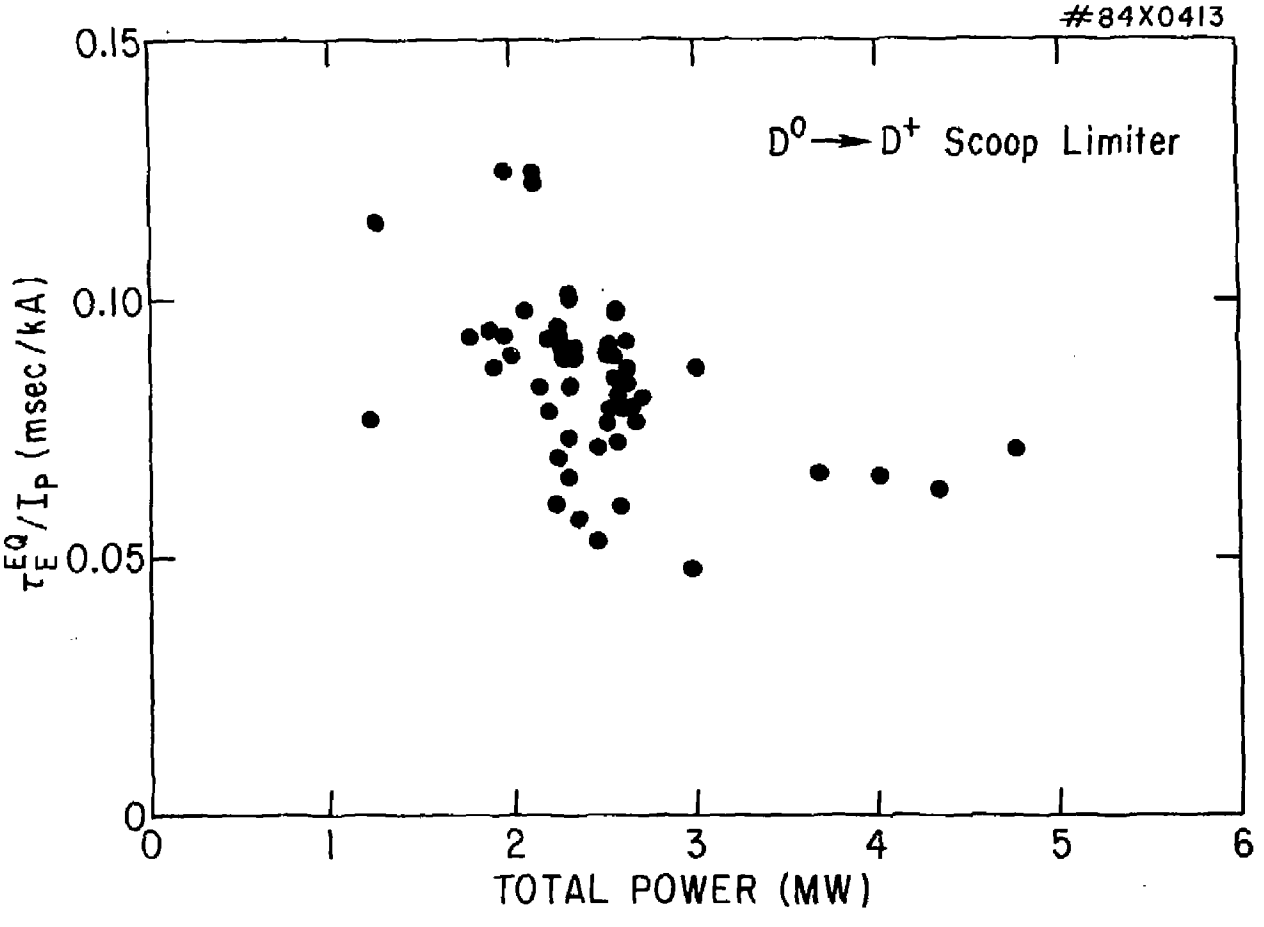
#84X0413
D⁰ → D⁺ Scoop Limiter
0.15
0.10
0.05
0
τ_E^{EQ}/I_p (msec/kA)
0
1
2
3
4
5
6
TOTAL POWER (MW)

Fig. 10

EXTERNAL DISTRIBUTION IN ADDITION TO TIC UC-20

Plasma Res Lab, Austre Nat'l Univ, AUSTRALIA
Dr. Frank J. Paoloni, Univ of Wollongong, AUSTRALIA
Prof. I.R. Jones, Flinders Univ., AUSTRALIA
Prof. M.H. Brennan, Univ Sydney, AUSTRALIA
Prof. F. Cap, Inst Theo Phys, AUSTRIA
Prof. Frank Verheest, Inst theoretische, BELGIUM
Dr. D. Palumbo, Dg XII Fusion Prog, BELGIUM
Ecole Royale Militaire, Lab de Phys Plasmas, BELGIUM
Dr. P.H. Sakanaka, Univ Estadual, BRAZIL
Dr. C.R. James, Univ of Alberta, CANADA
Prof. J. Teichmann, Univ of Montreal, CANADA
Dr. H.M. Skarsgard, Univ of Saskatchewan, CANADA
Prof. S.R. Sreenivasan, University of Calgary, CANADA
Prof. Tudor W. Johnston, INRS-Energie, CANADA
Dr. Hannes Barnard, Univ British Columbia, CANADA
Dr. M.P. Bachynski, MPB Technologies, Inc., CANADA
Zhengwu Li, SW Inst Physics, CHINA
Library, Tsing Hua University, CHINA
Librarian, Institute of Physics, CHINA
Inst Plasma Phys, Academia Sinica, CHINA
Dr. Peter Lukac, Komenskeho Univ, CZECHOSLOVAKIA
The Librarian, Culham Laboratory, ENGLAND
Prof. Schatzman, Observatoire de Nice, FRANCE
J. Radet, CEN-BP6, FRANCE
AM Dupas Library, AM Dupas Library, FRANCE
Dr. Tom Mual, Academy Bibliographic, HONG KONG
Preprint Library, Cent Res Inst Phys, HUNGARY
Dr. S.K. Trehan, Panjab University, INDIA
Dr. Indra, Mohan Lal Das, Banaras Hindu Univ, INDIA
Dr. L.K. Chavda, South Gujarat Univ, INDIA
Dr. R.K. Chhajlani, Var Ruchi Marg, INDIA
P. Kaw, Physical Research Lab, INDIA
Dr. Phillip Rosenau, Israel Inst Tech, ISRAEL
Prof. S. Cuperman, Tel Aviv University, ISRAEL
Prof. G. Rostagni, Univ Di Padova, ITALY
Librarian, Int'l Ctr Theo Phys, ITALY
Miss Clelia De Palo, Assoc EURATOM-CNEN, ITALY
Biblioteca, del CNR EURATOM, ITALY
Dr. H. Yamato, Toshiba Res & Dev, JAPAN
Prof. M. Yoshikawa, JAERI, Tokai Res Est, JAPAN
Prof. T. Uchida, University of Tokyo, JAPAN
Research Info Center, Nagoya University, JAPAN
Prof. Kyoji Nishikawa, Univ of Hiroshima, JAPAN
Prof. Sigeru Mori, JAERI, JAPAN
Library, Kyoto University, JAPAN
Prof. Ichiro Kawakami, Nihon Univ, JAPAN
Prof. Setoshi Itoh, Kyushu University, JAPAN
Tech Info Division, Korea Atomic Energy, KOREA
Dr. R. England, Ciudad Universitaria, MEXICO
Bibliotheek, Fom-Inst Voor Plasma, NETHERLANDS
Prof. B.S. Liley, University of Waikato, NEW ZEALAND
Dr. Suresh C. Sharma, Univ of Calabar, NIGERIA
Prof. J.A.C. Cabral, Inst Superior Tech, PORTUGAL
Dr. Octavian Petrus, ALI CUZA University, ROMANIA
Prof. M.A. Hellberg, University of Natal, SO AFRICA
Dr. Johan de Villiers, Atomic Energy Bd, SO AFRICA
Fusion Div. Library, JEN, SPAIN
Prof. Hans Wilhelmson, Chalmers Univ Tech, SWEDEN
Dr. Lennart Stenflo, University of UMEA, SWEDEN
Library, Royal Inst Tech, SWEDEN
Dr. Erik T. Karlson, Uppsala Universitet, SWEDEN
Centre de Recherchesen, Ecole Polytech Fed, SWITZERLAND
Dr. W.L. Weise, Nat'l Bur Stand, USA
Dr. W.M. Stacey, Georg Inst Tech, USA
Dr. S.T. Wu, Univ Alabama, USA
Prof. Norman L. Oleson, Univ S Florida, USA
Dr. Benjamin Ma, Iowa State Univ, USA
Prof. Magne Kristiansen, Texas Tech Univ, USA
Dr. Raymond Askew, Auburn Univ, USA
Dr. V.T. Tolok, Kharkov Phys Tech Ins, USSR
Dr. D.D. Ryutov, Siberian Acad Sci, USSR
Dr. G.A. Eliseev, Kurchatov Institute, USSR
Dr. V.A. Glukhikh, Inst Electro-Physical, USSR
Institute Gen. Physics, USSR
Prof. T.J. Boyd, Univ College N Wales, WALES
Dr. K. Schindler, Ruhr Universitat, W. GERMANY
Nuclear Res Estab, Julich Ltd, W. GERMANY
Librarian, Max-Planck Institut, W. GERMANY
Dr. H.J. Kaeppler, University Stuttgart, W. GERMANY
Bibliothek, Inst Plasmaforschung, W. GERMANY